Epsilon-Near-Zero Mode for Active Optoelectronic Devices

S. Vassant,[1,2] A. Archambault,[1] F. Marquier,[1] F. Pardo,[2] U. Gennser,[2] A. Cavanna,[2] J. L. Pelouard,[2] and J. J. Greffet[1]

[1]*Laboratoire Charles Fabry, Institut d'Optique, CNRS, Université Paris-Sud, 2 avenue Augustin Fresnel, 91127 Palaiseau cedex, France*

[2]*Laboratoire de Photonique et Nanostructures (LPN-CNRS), Route de Nozay, F-91460 Marcoussis, France*

(Received 3 May 2012; published 4 December 2012)

The electromagnetic modes of a GaAs quantum well between two AlGaAs barriers are studied. At the longitudinal optical phonon frequency, the system supports a phonon polariton mode confined in the thickness of the quantum well that we call epsilon-near-zero mode. This epsilon-near-zero mode can be resonantly excited through a grating resulting in a very large absorption localized in the single quantum well. We show that the reflectivity can be modulated by applying a voltage. This paves the way to a new class of active optoelectronic devices working in the midinfrared and far infrared at ambient temperature.

DOI: 10.1103/PhysRevLett.109.237401 PACS numbers: 85.60.−q, 42.79.Ta, 73.20.Mf, 78.68.+m

A cornerstone of nanophotonics is the enhancement of electron-photon interaction by combining field confinement and resonances as in microcavities or nanoantennas. This enhancement can also be obtained by using surface waves, e.g., surface plasmon or surface phonon polaritons (SPhPs) [1,2]. Examples of applications include the enhancement of Raman scattering [3], the enhancement of fluorescence [4,5], the enhancement of the radiative decay rate [6,7], and localized heating [8]. More recently, a further step was done by introducing active plasmonic devices [9–12]. In the infrared, SPhPs allow designing resonant absorbers as demonstrated with polar semiconductors in the infrared [13,14] and terahertz (THz) [15] ranges. However, it is more difficult to use surface waves to enhance interaction with electrons in a quantum well (QW), as their spatial extension is generally more than 1 order of magnitude larger than a typical QW thickness and therefore the electron-photon spatial overlap is far from optimum. We overcome this issue by the epsilon-near-zero (ENZ) effect, which has been discussed in a series of recent papers [16–19]. Here, we introduce an ENZ SPhP mode (hereafter called the ENZ mode), which allows enhancing the incident intensity by more than 2 orders of magnitude in a single QW. We first discuss the ENZ mode properties in the case of a single AlGaAs/GaAs/AlGaAs QW. We then demonstrate experimentally a resonant absorption due to the ENZ mode excitation. We finally report an electrical control of this absorption that allows modulating the reflectivity at ambient temperature.

Let us first introduce the ENZ mode. If one considers an interface between two media (1 and 2), the electric displacement $\epsilon_{zz}E_z$ normal to the interfaces is continuous so that $E_{z2}/E_{z1} = \epsilon_{zz1}/\epsilon_{zz2}$, where ϵ_{ij} is the diagonal complex dielectric tensor and E the electric field. Thus if $|\epsilon_{zz2}| \ll |\epsilon_{zz1}|$, the field in medium 2 is enhanced compared to the field in medium 1. We can define an enhancement factor $K_{\mathrm{ENZ}} = |E_{z2}/E_{z1}|^2 = |\epsilon_{zz1}/\epsilon_{zz2}|^2$. We now consider the $GaAs/Al_{0.33}Ga_{0.67}As$ system and show that it naturally exhibits ENZ enhancement. Our goal is to combine this effect with the resonant excitation of a SPhP to achieve a resonant absorption. In Fig. 1(a), we plot the real part of the dielectric function of GaAs. The green (dark gray) shaded area corresponds to $K_{\mathrm{ENZ}} \geq 50$, whereas the gray shaded area corresponds to the frequency range where GaAs and AlGaAs have the real part of their dielectric constants with opposite signs so that a SPhP can exist at a GaAs/AlGaAs interface. The ENZ and SPhP frequency range do not overlap for this geometry. However, if we consider a slab of GaAs embedded in AlGaAs [Fig. 1(c)], SPhPs propagating at both interfaces can couple, leading to a splitting of the SPhP dispersion relation in two branches [20]. As can be seen in Fig. 1(b), the splitting increases when the slab thickness (d) decreases.

For small thicknesses (here 22 nm), the frequency of the higher energy branch enters the ENZ frequency range but remains smaller than the longitudinal optical phonon frequency of GaAs ($\omega_{\mathrm{GaAs,LO}} \approx 291.55\ \mathrm{cm}^{-1}$ [20]), so that the condition $\mathrm{Re}[\epsilon_{\mathrm{GaAs}}(\omega)] < 0$ is fulfilled. We refer to this mode as the ENZ mode. Its field distribution is depicted in Fig. 1(c), for a GaAs thickness of 22 nm and a 7000 cm^{-1} wave vector. Two important features are seen: (i) The field is confined in the QW; (ii) the amplitude in GaAs is more than 1 order of magnitude larger than in $Al_{0.33}Ga_{0.67}As$. The system bears some resemblance to two surface plasmons propagating along a thin metallic film. In both cases, we have a metal-like medium embedded in a dielectric. The ENZ mode has the same field symmetry as the long-range surface plasmon (symmetric normal electric field) [21,22]. Despite these similarities, the ENZ mode and the long-range surface plasmon have significant differences: (i) a different field distribution-$|E|$ is maximum in the film for the ENZ mode, whereas it is minimum in the case of the long-range surface plasmon-and (ii) the ENZ mode dispersion relation is almost flat for a large range of wave vectors, with $\omega \approx \omega_{\mathrm{GaAs,LO}}$.

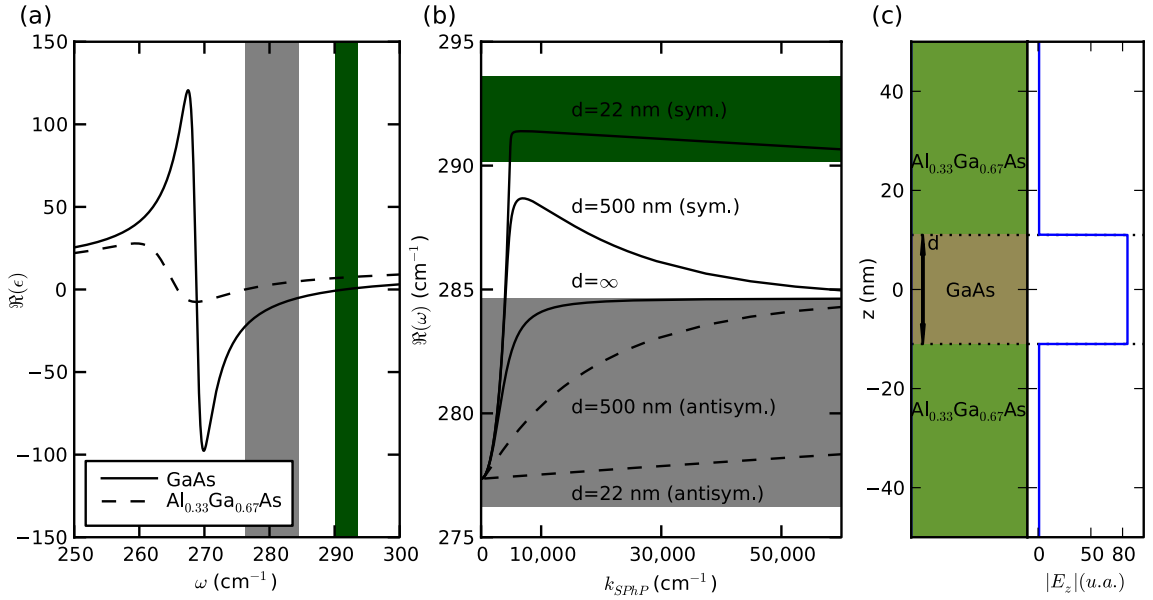

FIG. 1 (color online). (a) Real part of GaAs and $Al_{0.33}Ga_{0.67}As$ bulk dielectric functions as a function of the frequency. The gray area corresponds to the frequency range where a SPhP at the GaAs/$Al_{0.33}Ga_{0.67}As$ single interface can exist. The green (dark gray) shaded area corresponds to the ENZ regime of GaAs, defined by $K_{\mathrm{ENZ}} = |\epsilon_{zz\mathrm{AlGaAs}}/\epsilon_{zz\mathrm{GaAs}}|^2 \geq 50$. (b) Dispersion relation for the slab geometry and different GaAs thicknesses d. The gray and green (dark gray) shaded areas have the same meaning as in (a). When $d = \infty$, the system is similar to a single interface geometry. As the thickness is decreased, the mode separates into two branches (symmetric and antisymmetric normal electric field distribution [21,22]). When $d = 22$ nm, the symmetric branch frequency enters the ENZ regime of GaAs. (c) Left: $Al_{0.33}Ga_{0.67}As$/GaAs/$Al_{0.33}Ga_{0.67}As$ slab geometry; right: spatial distribution of the z-electric field component of the ENZ mode at 34.3 μm for a wave vector of 7000 cm^{-1} and a GaAs thickness d of 22 nm.

We now show how the ENZ mode can be used for optoelectronic devices. Here, we limit the discussion to the electrical control of THz reflectivity. Other THz modulation schemes have already been demonstrated [23–26], but they encounter certain difficulties when working at higher frequency [27] and do not work in the optical phonon frequency range of their constitutive materials. Using optical phonons for optoelectronic devices can be surprising, as they are usually considered to be detrimental. Indeed, the electron–optical-phonon interaction is a relaxation process much faster than the electron-photon interaction at work in most optoelectronics devices. Here, we use a different scheme based on the resonant absorption by the ENZ mode. Electrons are not used to absorb light but to modulate the ENZ effect. The principle is summarized here: Incident light is coupled through a grating to the ENZ mode, leading to a resonant absorption so that energy is finally dissipated as heat. The GaAs layer thickness is adjusted to 22 nm to form a QW where one intersubband transition (ISBT) energy is close to that of the ENZ mode. Thanks to the ISBT, the z component of the QW dielectric tensor (see Ref. [20] for details) depends on the electron density in the well and can be tuned by a gate voltage. This gives an electrical control of the ENZ enhancement and thus of the absorption, as a lower ENZ enhancement leads to a smaller absorption.

The device is depicted in Fig. 2(a). The incident THz field is coupled to the ENZ mode by a grating made of gold stripes which also serves as a Schottky gate for electrical control of the electron density in the single 22 nm thick GaAs QW. The substrate is a doped GaAs wafer, which behaves as a back-mirror at THz frequencies. The grating features and spacer thickness were chosen to optimize the absorption in the depleted QW through numerical simulations [20]. Details about the fabrication can be found in Ref. [20]. Reflectivity spectra [20], with a p-polarized incident wave [Fig. 2(b)], show that a 76% absorption is achieved at 34.3 μm (corresponding to the longitudinal optical phonon frequency 8.74 THz) when a negative gate voltage is applied. This bias depletes the QW, so that the ISBT contribution to the dielectric constant vanishes. No absorption is observed for s polarization [20]. Numerical simulations using bulk dielectric constants agree well with the reflectivity data [Fig. 2(b)]. Moreover, they show that 45% of the incident energy is absorbed within the QW by the ENZ mode. The remaining 31% is absorbed in the rest of the structure. The calculated near field distribution at resonance confirms the strong $|E_z|^2$ enhancement confined in the QW (Fig. 3). Figure 2(c) shows that the resonant absorption does not depend on the angle, as expected from the almost flat dispersion relation of the ENZ mode. It is worth comparing this 45% absorption by the ENZ mode in a single QW with the intersubband absorption of a quantum well infrared photodetector consisting of 50 QWs, which is typically less than 25% [28]. Furthermore, we

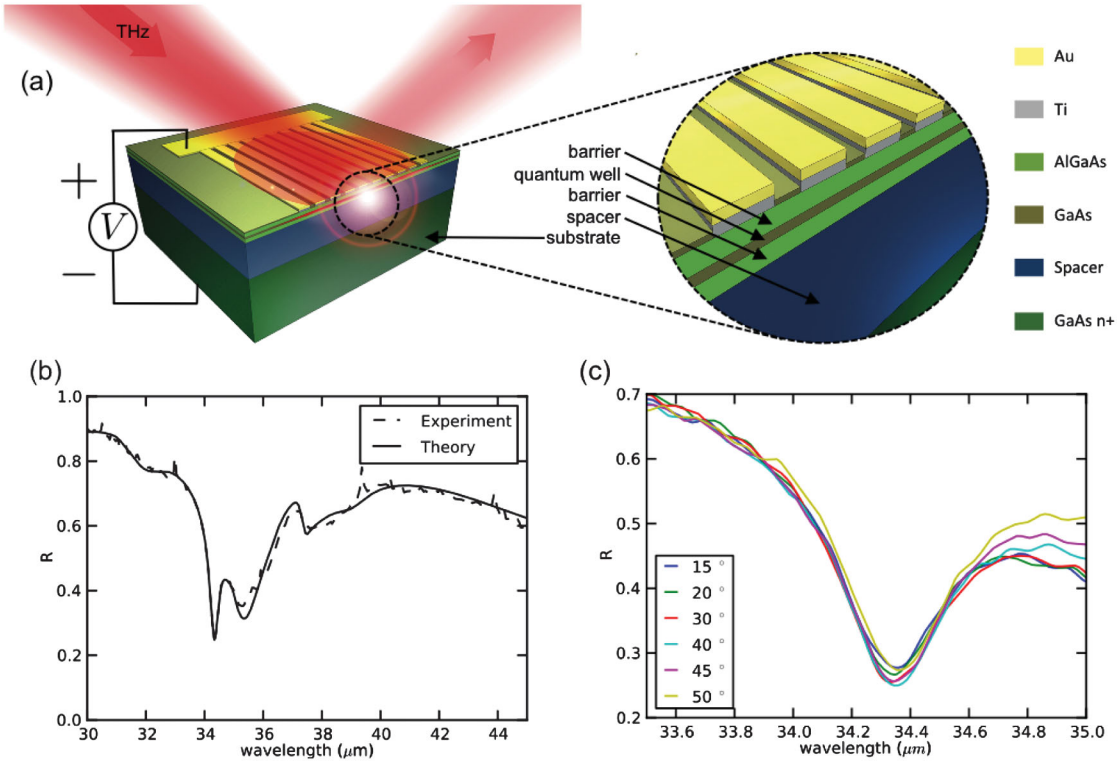

FIG. 2 (color). Excitation of the ENZ mode. (a) Scheme of the device made of a gold lamellar grating with 4 μm period, 200 nm thickness, a 0.66 filling factor, a 22 nm GaAs quantum well buried in $Al_{0.33}Ga_{0.67}As$ barriers, a 1300 nm $Al_{0.5}Ga_{0.5}As$ spacer [20], and a doped GaAs substrate. (b) Reflectivity spectrum for a p-polarized incident wave incident at 15°, with an applied gate voltage of $V = -0.3$ V, data and theory. An absorption peak appears at 34.31 μm. The incident wave is p-polarized. Note that the second absorption peak near 36 μm is due to a surface plasmon propagating on the top of the metallic grating [20]. (c) Reflectivity for various angles of incidence for an applied voltage of $V = -0.3$ V. The absorption peak is almost independent on the angle of incidence. The reflectivity changes as a function of the angle of incidence above 34.6 μm are discussed in Ref. [20].

did calculations on the same structure without a grating and found a maximum absorption in the QW of 4%, only at the Brewster angle.

We now turn to the modulation of the reflectivity. Experimental reflectivity spectra at room temperature for different gate voltages are shown in Fig. 4(a). It is seen that at the resonance (34.3 μm) the reflectivity decays from 0.38 to 0.25 when the applied voltage goes from +0.3 to −0.3 V. The corresponding relative variation is as large as 54%, as displayed in Fig. 4(b). For larger voltages, the reflectivity change tends to saturate. The physical mechanism is based on controlling the ENZ effect with ISBT in the QW. As previously pointed out, we have an ISBT at the frequency of the ENZ mode (see Ref. [20] for more details). An increase of the electron density, through an increase of the gate voltage (− 0.3 to +0.3 V) between the metallic grating and the doped substrate, increases the imaginary part of the intersubband contribution to the dielectric constant at the interface mode frequency. Hence ϵ_{zzGaAs} is no longer close to zero, resulting in a suppression of the ENZ field enhancement. By fitting the experimental reflectivity spectrum, we obtain the values for the dielectric function for various electronic densities

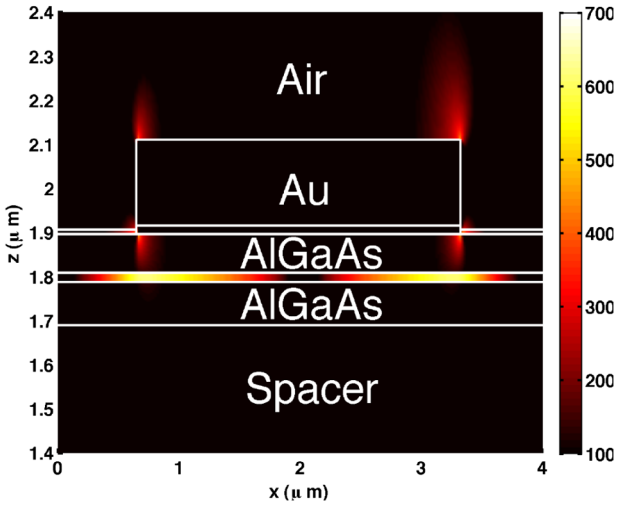

FIG. 3 (color online). Normalized near field distribution $|E_z|^2$ at the resonance (34.3 μm) for a p-polarized plane wave incident at 15° on the structure. The white lines represent the geometry. Only one period of the grating is represented.

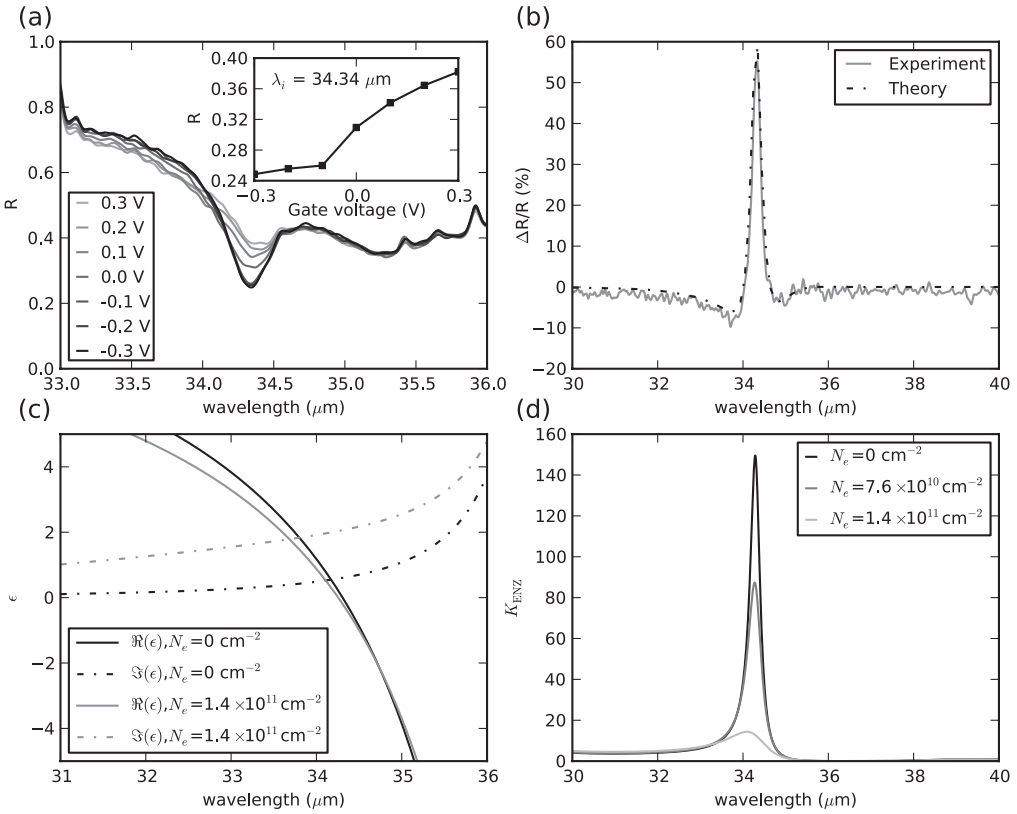

FIG. 4. Electrical modulation of the reflectivity. (a) TM reflectivity for different applied voltages for an angle of incidence of 15°. The inset shows the evolution of the reflectivity at 34.31 μm as a function of the gate voltage. (b) Corresponding relative reflectivity modulation between -0.3 and $+0.3$ V, data and theory. (c) Dielectric function of GaAs without (electronic density Ne $= 0$ cm^{-2}) and with ISBT (Ne $= 1.4 \times 10^{11}$ cm^{-2}, $\gamma_{\mathrm{isb}} = 330$ fs). (d) ENZ enhancement factor K_{ENZ} as a function of the electronic density in the QW.

[20] [Fig. 4(c)] and calculate the corresponding K_{ENZ} factor that strongly decreases as the electronic density in the QW increases [Fig. 4(d)]. For practical applications, the time response of the device is an important figure of merit. We estimate [20] the maximum bandwidth, mainly limited by the capacitance of the device, to be on the order of 1 GHz. Note that the maximum electrical power flowing through the device is 425 nW at $+0.3$ V so that thermal effects are negligible [20].

In summary, we have introduced an ENZ mode that exhibits strong field enhancement. It can be used to engineer large absorption in a layer as thin as 22 nm ($\approx \lambda_i/1560$). The strong interaction between the ENZ mode and the bidimensional electron gas allows controlling electrically the absorption. A relative change in the reflectivity up to 54% is experimentally obtained at 8.74 THz and room temperature with a single AlGaAs/GaAs/AlGaAs QW. The ENZ effect is limited to a narrow range of wavelengths for a given material system but is present in all polar crystals [29]. As a result this effect can be used at various wavelengths such as 11 μm in SiC, or 13.5 μm with GaN, where the existing modulation scheme becomes challenging. The control of the ENZ effect appears to be a very promising mechanism to enhance light-matter interaction at the nanoscale. Due to Kirchhoff's law, enhancing and controlling the absorption means that emission can also be enhanced and controlled. Enhancing the ENZ mode electron interaction suggests that electrical transport measurements in the QW should allow the detection of incident radiation. Hence, using the ENZ mode opens new avenues for the design of modulators, sources, and detectors.

This work has been supported by RTRA through Project No. PAO 2008-057T, the ANR contract LAPSUS and by the region Ile de France through a C'Nano Idf project. We thank G. Morisseau for his help with the illustrations.

[1] W. L. Barnes, A. Dereux, and T. W. Ebbesen, Nature (London) **424**, 824 (2003).
[2] J. A. Schuller, E. S. Barnard, W. Cai, Y. Chul Jun, J. S. White, and M. L. Brongersma, Nat. Mater. **9**, 193 (2010).
[3] S. Nie and S. R. Emory, Science **275**, 1102 (1997).
[4] P. Anger, P. Bharadwaj, and L. Novotny, Phys. Rev. Lett. **96**, 113002 (2006).
[5] S. Kühn, U. Hakanson, L. Rogobete, and V. Sandoghdar, Phys. Rev. Lett. **97**, 017402 (2006).
[6] K. H. Drexhage, H. Kuhn, and F. P. Schäfer, Ber. Bunsen-Ges. Phys. Chem. **72**, 329 (1968); **70**, 1179 (1966).

[7] R. R. Chance, A. Prock, and R. Silbey, J. Chem. Phys. **60**, 2744 (1974).
[8] W. A. Challener, C. Peng, A. V. Itagi, D. Karns, W. Peng, Y. Peng, X. Yang, X. Zhu, N. J. Gokemeijer, Y.-T. Hsia, G. Ju, R. E. Rottmayer, M. A. Seigler, and E. C. Gage, Nat. Photonics **3**, 220 (2009).
[9] K. Hassan, J.-C. Weeber, L. Markey, A. Dereux, A. Pitilakis, O. Tsilipakos, and E. E. Kriezis, Appl. Phys. Lett. **99**, 241110 (2011).
[10] M. A. Noginov, G. Zhu, A. M. Belgrave, R. Bakker, V. M. Shalaev, E. E. Narimanov, S. Stout, E. Herz, T. Suteewong, and U. Wiesner, Nature (London) **460**, 111D0 (2009).
[11] R. F. Oulton, V. J. Sorger, T. Zentgraf, R.-M. Ma, C. Gladden, L. Dai, G. Bartal, and X. Zhang, Nature (London) **461**, 629 (2009).
[12] I. De Leon and P. Berini, Nat. Photonics **4**, 382 (2010).
[13] J. J. Greffet, R. Carminati, K. Joulain, J.-P. Mulet, S. Mainguy, and Y. Chen, Nature (London) **416**, 61 (2002).
[14] F. Marquier, K. Joulain, J.-P. Mulet, R. Carminati, J. J. Greffet, and Y. Chen, Phys. Rev. B **69**, 155412 (2004).
[15] S. Vassant, F. Marquier, J. J. Greffet, F. Pardo, and J.-L. Pelouard, Appl. Phys. Lett. **97**, 161101 (2010).
[16] S. Enoch, G. Tayeb, P. Sabouroux, N. Guérin, and P. Vincent, Phys. Rev. Lett. **89**, 213902 (2002).
[17] M. Silveirinha and N. Engheta, Phys. Rev. Lett. **97**, 157403 (2006).
[18] B. Edwards, A. Alu, M. E. Young, M. Silveirinha, and N. Engheta, Phys. Rev. Lett. **100**, 033903 (2008).
[19] N. M. Litchinitser, A. I. Maimistov, I. R. Gabitov, R. Z. Sagdeev, and V. M. Shalaev, Opt. Lett. **33**, 2350 (2008).
[20] See Supplemental Material at http://link.aps.org/supplemental/10.1103/PhysRevLett.109.237401 for details on dispersion relation and reflectivity numerical calculations, sample fabrication, experimental setup, and complementary measurements as well as bandwidth and thermal considerations.
[21] D. Sarid, Phys. Rev. Lett. **47**, 1927 (1981).
[22] P. Berini, Adv. Opt. Photon. **1**, 484 (2009).
[23] R. Kersting, G. Strasser, and K. Unterrainer, Electron. Lett. **36**, 1156 (2000).
[24] T. Kleine-Ostmann, P. Dawson, K. Pierz, G. Hein, and M. Koch, Appl. Phys. Lett. **84**, 3555 (2004).
[25] H. Chen, W. J. Padilla, J. M. O. Zide, A. C. Gossard, A. J. Taylor, and R. D. Averitt, Nature (London) **444**, 597 (2006).
[26] W. Maineult, L. Ding, P. Gellie, P. Filloux, C. Sirtori, S. Barbieri, T. Akalin, J.-F. Lampin, I. Sagnes, H. E. Beere, and D. A. Ritchie, Appl. Phys. Lett. **96**, 021108 (2010).
[27] A. Gabbay, J. Reno, J. R. Wendt, A. Gin, M. C. Wanke, M. B. Sinclair, E. Shaner, and I. Brener, Appl. Phys. Lett. **98**, 203103 (2011).
[28] B. F. Levine, J. Appl. Phys. **74**, R1 (1993).
[29] All crystalline materials with more than two different atoms per unit cell are polar and have at least one infrared active optical phonon. In particular, compounds and alloy made of I–VII, II–VI, III–V, and IV–IV materials are polar.